

C.P. No. 665

BEDFORD.

C.P. No. 665



MINISTRY OF AVIATION

AERONAUTICAL RESEARCH COUNCIL

CURRENT PAPERS

A Note on the Generalisation
of Elastic Curves Representing
Parachute Shapes

by

W. G. S. Lester, M.A., D.Phil.

LONDON: HER MAJESTY'S STATIONERY OFFICE

1963

PRICE 6s 6d NET

A NOTE ON THE GENERALISATION OF ELASTIC CURVES
REPRESENTING PARACHUTE SHAPES

by

W. G. S. Lester, M.A., D.Phil.

SUMMARY

The Note gives a concise treatment of the theory of parachute canopy shapes and stresses. An analysis is made of the equation

$$\sin \varphi = \frac{1}{\lambda} \left[\lambda - 1 + \frac{r^2}{a^2} \right]$$

where r is the radial distance measured from the axis of symmetry and a its maximum value; φ is the angle the tangent to the curve makes with a plane normal to the axis of symmetry and λ is a parameter. By varying λ a family of elastic curves is generated representing the shapes of flat, conical and annular parachutes and also those with an axial cord. General equations for calculating the fabric surface area and canopy volume in the solid fabric construction are included, together with equations for determining the gore shapes for both the cords over canopy and solid fabric constructions. An approximate analysis is given of the stress distribution in the two constructions. A parachute with an axial cord is shown to have the minimum bulk for a given inflated diameter but its merit on other parachute requirements is doubtful. Experiments are suggested to relate canopy shape and volume with stability and a deep conical parachute is thought to have several desirable stability characteristics.

LIST OF CONTENTS

	<u>Page</u>
1 INTRODUCTION	3
2 PRELIMINARY ANALYSIS	4
2.1 The case $\lambda \geq \frac{1}{2}$	5
2.2 The case $0 < \lambda \leq \frac{1}{2}$	7
3 THE SOLID FABRIC CONSTRUCTION	9
3.1 Stresses in the fabric	10
3.2 The surface area of the fabric	14
3.3 The volume enclosed by the canopy	16
4 THE CORDS OVER CANOPY DESIGN	17
5 CONCLUSIONS	20
LIST OF SYMBOLS	20
LIST OF REFERENCES	21
APPENDICES 1 AND 2	23-25
TABLES 1 AND 2	25-26
ILLUSTRATIONS - Fig.1-4	-
DETACHABLE ABSTRACT CARDS	-

LIST OF APPENDICES

Appendix

1 - Elliptic integrals	23
2 - Canopy, cord and gore coordinates	25

LIST OF TABLES

Table

1 - Coordinates for canopies with $\lambda > \frac{1}{2}$	25
2 - Coordinates for canopies with $0 < \lambda < \frac{1}{2}$	26

LIST OF ILLUSTRATIONS

	<u>Fig.</u>
Diagrams showing the notation used when (a) $\lambda > \frac{1}{2}$ and (b) $0 < \lambda < \frac{1}{2}$	1(a)&(b)
Canopy shapes for $\lambda > \frac{1}{2}$	2
Canopy shapes for $0 < \lambda < \frac{1}{2}$	3
Gore shapes for the solid fabric construction	4

1 INTRODUCTION

During the investigation of the equilibrium configurations assumed by some rotationally symmetric fabric structures subjected to certain forms of loading and with a constant pressure difference across the fabric it was found that the shapes could be represented by an equation of the form

$$\sin \varphi = \frac{1}{\lambda} \left[\lambda - 1 + \frac{r^2}{a^2} \right]. \quad (1)$$

In this equation r is the radial distance measured from the axis of symmetry and a is its maximum value occurring when $\varphi = \pi/2$; φ is the angle the tangent to the curve at a point distant r from the axis of symmetry makes with a plane normal to that axis and λ is a parameter. By varying the parameter λ a family of curves is generated, identical with the elastica occurring in the theory of the buckling of columns and struts as originally investigated by Euler.

The following examples show the range of shapes arising in parachute theory and which can be represented by equation (1):

(i) With $\lambda = 1$ the equation becomes

$$\sin \varphi = \frac{r^2}{a^2} \quad (2)$$

which gives the well-known Taylor shape; in a solid fabric construction it is the shape theoretically taken up by a parachute when the fabric is about to crinkle and the tension in the circumferential direction is zero¹; for the design with cords over the canopy it represents the shape taken up by the cords².

(ii) With λ such that $\frac{1}{2} < \lambda < 1$ equation (1) represents the shape of the parachute with an axial cord and zero circumferential tension in a solid construction³; it also represents the shape of the cords for the corresponding design with cords over the canopy⁴.

(iii) With $\lambda > 1$ the equation gives a family of conical shapes very similar to the conical parachute, although as far as the writer is aware no use of this has been made for design purposes.

(iv) With $0 < \lambda < \frac{1}{2}$ the curve does not meet the axis of symmetry and can be used to represent an annular parachute; again no use has been made of this in design.

(v) In the theory of some inflatable lifting structures the whole range of values of λ is encountered⁵.

From these examples it is evident that equation (1) is of considerable interest and a general investigation of its properties is of value for both design purposes and in studies of canopy shapes and stresses.

In earlier work associated with particular values of λ it has been usual to determine the arc length s in terms of φ , to give the intrinsic equation, and to obtain the distance x measured along the axis of symmetry, thus making it possible to plot the particular curves. The transfer to

cylindrical coordinates is not difficult but can be made to appear unduly complicated by retaining λ in terms of certain geometric conditions and not using a portmanteau symbol (e.g. Ref.4). When treated generally the equation is quite easy to study although the information extracted is mostly in terms of elliptic integrals. For the benefit of those who are not familiar with these integrals it should be remarked that for the purposes of this Note the only parts of the theory required are to be found in the elementary sections of any of the standard texts on the subject (e.g. Refs.6 and 7).

The object of this Note is to present an analysis of equation (1) in as simple a form as possible; to consider the stress distribution for different values of λ in a solid fabric construction; and to give the methods for deriving the gore shape for both the solid fabric and cords over canopy designs. The Note does not pretend to present any particularly original matter, the design of parachutes of the shaped gore and cords over canopy type is well-established, as is that for the parachute with an axial cord; however, this theory does not appear to have been applied to either the conical or the annular parachute. The fact that all these types of parachute can be described by one equation involving a parameter has not been realised; it is convenient to discuss the equation generally as a concise summary of the theory of parachute shapes has not been given previously and many of the original papers dealing with particular cases are not readily available.

2 PRELIMINARY ANALYSIS

Consider equation (1):

$$\sin \varphi = \frac{1}{\lambda} \left[\lambda - 1 + \frac{r^2}{a^2} \right].$$

It is known that $|\sin \varphi| \leq 1$ and hence

$$\left| \frac{1}{\lambda} \left[\lambda - 1 + \frac{r^2}{a^2} \right] \right| \leq 1.$$

For this to be satisfied

$$0 \leq \frac{1}{\lambda} \left(1 - \frac{r^2}{a^2} \right) \leq 2. \quad (3)$$

Hence, for $\frac{r^2}{a^2} \leq 1$,

$$\lambda > 0. \quad (4)$$

If the curve given by (1) is to meet the axis of symmetry ($r = 0$) the inequality (3) must be valid for all $r \leq a$ which implies that

$$\lambda \geq \frac{1}{2}.$$

With $0 < \lambda < \frac{1}{2}$ the curve can only exist for values of r such that

$$\frac{r^2}{a} > 1 - 2\lambda . \quad (5)$$

It is apparent that separate consideration must be given to the cases where $0 < \lambda < \frac{1}{2}$ and $\lambda \geq \frac{1}{2}$.

2.1 The case $\lambda \geq \frac{1}{2}$

Suppose we take as origin O one of the points where the curve meets the axis of symmetry and measure distance x along this axis and arc length s along the curve from O . (See Fig.1a) Now, using ordinary differential geometric relations

$$ds = \frac{dr}{\cos \phi} \quad (6)$$

and on substituting from equation (1) and integrating between appropriate limits

$$\frac{s}{a} = \int_0^{r/a} \frac{\lambda d\left(\frac{r}{a}\right)}{\sqrt{\left\{1 - \left(\frac{r}{a}\right)^2\right\} \left\{2\lambda - 1 + \left(\frac{r}{a}\right)^2\right\}}} . \quad (7)$$

This integral can be expressed in the standard form (i) given in Appendix 1 when the range of integration is separated so that the upper limits are unity i.e.

$$\int_0^{r/a} f d\left(\frac{r}{a}\right) = \int_0^1 f d\left(\frac{r}{a}\right) - \int_{\frac{r}{a}}^1 f d\left(\frac{r}{a}\right) ;$$

the result is

$$\frac{s}{a} = \sqrt{\left(\frac{\lambda}{2}\right)} \left\{ F \left[\frac{\pi}{2}, \sqrt{\left(\frac{1}{2\lambda}\right)} \right] - F \left[\cos^{-1} \left(\frac{r}{a} \right), \sqrt{\left(\frac{1}{2\lambda}\right)} \right] \right\} . \quad (8)$$

In equation (8) $F[\theta, k]$ is the Legendre elliptic integral of the first kind with argument θ and modulus k .

For the coordinate x the geometric relations give

$$dx = \sin \phi ds = \frac{\sin \phi}{\cos \phi} dr \quad (9)$$

and substituting in this from equation (1) and integrating between appropriate limits the following expression is obtained:-

$$\begin{aligned} \frac{x}{a} &= \int_0^{r/a} \frac{\left\{ \lambda - 1 + \left(\frac{r}{a}\right)^2 \right\} d\left(\frac{r}{a}\right)}{\sqrt{\left\{ 1 - \left(\frac{r}{a}\right)^2 \right\} \left\{ 2\lambda - 1 + \left(\frac{r}{a}\right)^2 \right\}}} \\ &= \int_0^{r/a} \sqrt{\frac{2\lambda - 1 + \left(\frac{r}{a}\right)^2}{1 - \left(\frac{r}{a}\right)^2}} d\left(\frac{r}{a}\right) - \int_0^{r/a} \frac{\lambda d\left(\frac{r}{a}\right)}{\sqrt{\left\{ 1 - \left(\frac{r}{a}\right)^2 \right\} \left\{ 2\lambda - 1 + \left(\frac{r}{a}\right)^2 \right\}}} . \quad (10) \end{aligned}$$

Separating the range of integration as before the integrals in (10) are again standard forms and on evaluation:

$$\begin{aligned} \frac{x}{a} &= \sqrt{2\lambda} \left\{ E\left(\frac{\pi}{2}, \sqrt{\frac{1}{2\lambda}}\right) - E\left(\cos^{-1}\left(\frac{r}{a}\right), \sqrt{\frac{1}{2\lambda}}\right) \right\} \\ &\quad - \sqrt{\frac{\lambda}{2}} \left\{ F\left(\frac{\pi}{2}, \sqrt{\frac{1}{2\lambda}}\right) - F\left(\cos^{-1}\left(\frac{r}{a}\right), \sqrt{\frac{1}{2\lambda}}\right) \right\} . \quad (11) \end{aligned}$$

In equation (11) $E[\theta, k]$ is the Legendre elliptic integral of the second kind with argument θ and modulus k .

To obtain the appropriate ranges for the arguments involved set

$$\cos^{-1}\left(\frac{r}{a}\right) = \xi = \cos^{-1} \sqrt{(\lambda \sin \varphi + 1 - \lambda)} , \quad (12)$$

then for

$$-\frac{\pi}{2} < \sin^{-1}\left(\frac{\lambda-1}{\lambda}\right) \leq \varphi \leq \frac{\pi}{2} :$$

$$\frac{\pi}{2} \geq \xi \geq 0$$

where $\xi = \frac{\pi}{2}$ corresponds to $\varphi = \sin^{-1}\left(\frac{\lambda-1}{\lambda}\right)$

(which is the angle the curve makes with the axis of symmetry when $r = 0$),

and $\xi = 0$ corresponds to $\varphi = \frac{\pi}{2}$;

$$\text{for } \varphi \geq \frac{\pi}{2} : \quad 0 \geq \xi \geq -\frac{\pi}{2}$$

$$\text{where } \xi = 0 \quad \text{corresponds to} \quad \varphi = \frac{\pi}{2}$$

$$\text{and } \xi = -\frac{\pi}{2} \quad \text{corresponds to} \quad \varphi = \pi - \sin^{-1}\left(\frac{\lambda-1}{\lambda}\right).$$

Equation (11) enables the curves for $\lambda \geq \frac{1}{2}$ to be plotted in the cylindrical coordinates r and x , using a set of tables of elliptic integrals, e.g. Ref.8. The coordinates for a range of values of λ are given in Appendix 2 and the curves are shown plotted in Fig.2. These curves are for values of λ corresponding to values of $\sin^{-1}k$ at intervals of 5° from 25° ($\lambda = 2.799$) to 60° ($\lambda = 0.6667$), and intervals of 10° from 60° to 80° ($\lambda = 0.5156$). The elliptic integrals are commonly tabulated with $\sin^{-1}k$ at intervals of 5° , to plot the curves for intermediate values of λ more complete tables are required than those of Ref.8; the tables of Ref.9 give $\sin^{-1}k$ at intervals of 1° and are probably the best available. The coordinates given include those for the values of λ corresponding to $\sin^{-1}k = 46^\circ, 47^\circ$ and 48° although, to avoid confusion, these have not been plotted in Fig.2.

2.2 The case $0 < \lambda < \frac{1}{2}$

When $0 < \lambda < \frac{1}{2}$ the curve does not meet the axis of symmetry; arc length is measured along the curve where it exists from an arbitrary point P say, where $r = r_1$, to a point Q where $r = r$, and the coordinate x is measured along the axis of symmetry from the point where the plane through P normal to this axis meets it, as is shown in Fig.1b.

In this case

$$\frac{s}{a} = \int_{r_1/a}^{r/a} \frac{\lambda d\left(\frac{r}{a}\right)}{\sqrt{\left\{1 - \left(\frac{r}{a}\right)^2\right\} \left\{\left(\frac{r}{a}\right)^2 - (1 - 2\lambda)\right\}}}. \quad (13)$$

Separating the range of integration so that

$$\int_{r_1/a}^{r/a} f d\left(\frac{r}{a}\right) = \int_{r_1/a}^1 f d\left(\frac{r}{a}\right) - \int_{r/a}^1 f d\left(\frac{r}{a}\right)$$

and using the appropriate standard form of Appendix 1, evaluation of the integral (13) leads to:-

$$\frac{s}{a} = \lambda \left\{ F(\zeta_1, \sqrt{2\lambda}) - F(\zeta, \sqrt{2\lambda}) \right\} \quad (14)$$

where

$$\zeta = \cos^{-1} \left\{ \frac{\left(\frac{r}{a}\right)^2 - (1 - 2\lambda)}{2\lambda} \right\}^{\frac{1}{2}} \quad (15)$$

and the suffix '1' refers to 'r' = r₁.

Similarly:

$$\frac{x}{a} = \int_{r_1/a}^{r/a} \frac{\left\{ \lambda - 1 + \left(\frac{r}{a}\right)^2 \right\} d\left(\frac{r}{a}\right)}{\sqrt{\left\{ 1 - \left(\frac{r}{a}\right)^2 \right\} \left\{ \left(\frac{r}{a}\right)^2 - (1 - 2\lambda) \right\}}} \quad (16)$$

and integrating by means of the standard forms (iii) and (iv) of Appendix 1,

$$\frac{x}{a} = E(\zeta_1, \sqrt{2\lambda}) - E(\zeta, \sqrt{2\lambda}) - (1 - \lambda) \{ F(\zeta_1, \sqrt{2\lambda}) - F(\zeta, \sqrt{2\lambda}) \}. \quad \dots (17)$$

For the appropriate ranges of the arguments involved set

$$\zeta = \cos^{-1} \left\{ \frac{\left(\frac{r}{a}\right)^2 - (1 - 2\lambda)}{2\lambda} \right\}^{\frac{1}{2}} = \cos^{-1} \left\{ \frac{1 + \sin \phi}{2} \right\}^{\frac{1}{2}},$$

then for

$$-\frac{\pi}{2} \leq \phi \leq \frac{\pi}{2} :$$

$$\frac{\pi}{2} \geq \zeta \geq 0$$

where $\zeta = \frac{\pi}{2}$ corresponds to $\phi = -\frac{\pi}{2}$

and $\zeta = 0$ corresponds to $\phi = \frac{\pi}{2}$;

$$\text{for } \varphi \geq \frac{\pi}{2} : \quad 0 \geq \zeta \geq -\frac{\pi}{2}$$

$$\text{where } \zeta = 0 \quad \text{corresponds to } \varphi = \frac{\pi}{2}$$

$$\text{and } \zeta = -\frac{\pi}{2} \quad \text{corresponds to } \varphi = \frac{3\pi}{2} .$$

The coordinates for some values of λ are given in Appendix 2 and the curves shown in Fig.3. Figs.2 and 3 now show the wide range of shapes which equation (1) represents and the curves for intermediate values of λ can be obtained using equations (11) and (17) and suitable tables of elliptic integrals.

3 THE SOLID FABRIC CONSTRUCTION

In this form of construction the canopy is made up of a number of gores cut from a plane sheet of fabric and seamed together. It is assumed that, when inflated, the whole canopy forms a surface of revolution and the gores do not bulge outward from the seams running between the apex and the peripheral hem; in practice the gore fabric does tend to bulge outwards and the theory of the stress distribution given can only be regarded as providing an approximate guide.

With n gores the width of each at distance r from the axis is $2\pi r/n$ and the length of the gore is s measured from either the canopy vertex or a suitable origin. The tables of Appendix 2 give corresponding values of r/a , s/a and x/a for a range of values of λ and it is a simple matter to determine the gore shape for a given 'n' and λ from these. A few gore shapes are shown in Fig.4.

If it is desired the width of the gore at a given distance s from the vertex or origin can be derived as follows:-

$$\text{Let} \quad \frac{r}{a} = \text{cn} \left(u, \sqrt{\frac{1}{2\lambda}} \right) \quad (18)$$

where $\text{cn}(u, k)$ is the elliptic function usually denoted by those symbols and $\lambda \geq \frac{1}{2}$. Then

$$u = F \left(\xi, \sqrt{\frac{1}{2\lambda}} \right)$$

and in equation (8)

$$\frac{s}{a} = \sqrt{\frac{\lambda}{2}} (K - u)$$

$$\text{where} \quad K = F \left(\frac{\pi}{2}, \sqrt{\frac{1}{2\lambda}} \right) .$$

Hence

$$u = K - \sqrt{\frac{2}{\lambda}} \frac{s}{a}$$

and in (18)

$$\frac{r}{a} = \operatorname{cn} \left\{ K - \sqrt{\frac{2}{\lambda}} \frac{s}{a}, \sqrt{\frac{1}{2\lambda}} \right\}.$$

Thus the width of the gore at distance s from the vertex of the canopy is

$$2w = \frac{2\pi a}{n} \operatorname{cn} \left\{ K - \sqrt{\frac{2}{\lambda}} \frac{s}{a}, \sqrt{\frac{1}{2\lambda}} \right\} \quad (19)$$

where w is the semi-gore width and $\lambda \geq \frac{1}{2}$.

For the cases where $0 < \lambda < \frac{1}{2}$ the gore width is still $2\pi r/n$ and a similar analysis to that of the previous paragraph enables one to determine the gore width for a given arc length s .

$$\text{Let } \left\{ \frac{\left(\frac{r}{a}\right)^2 - (1 - 2\lambda)}{2\lambda} \right\}^{\frac{1}{2}} = \operatorname{cn}(u, \sqrt{2\lambda}). \quad (20)$$

Then, from (14):

$$\frac{s}{a} = \lambda[u_1 - u]$$

where $u_1 = F(\zeta_1, \sqrt{2\lambda})$, and thus

$$u = u_1 - \frac{1}{\lambda} \frac{s}{a}. \quad (21)$$

The width of the gore at distance s from the position where $r = r_1$ is then

$$2w = \frac{2\pi a}{n} \left\{ 2\lambda \operatorname{cn}^2 \left(u_1 - \frac{1}{\lambda} \frac{s}{a}, \sqrt{2\lambda} \right) + (1 - 2\lambda) \right\}^{\frac{1}{2}} \quad (22)$$

where

$$0 < \lambda < \frac{1}{2}.$$

3.1 Stresses in the fabric

In the solid fabric construction the stresses in the fabric can be obtained using ordinary thin membrane theory. Regarding the canopy as a surface of revolution and supposing that the tension in the generator

direction is T_1 and in the circumferential or hoop direction is T_2 , it can be shown (c.f. Ref.1) that

$$\frac{d}{dr} (r T_1) = T_2 \quad (23)$$

and

$$T_1 r \frac{d}{dr} (\sin \varphi) + T_2 \sin \varphi = pr \quad (24)$$

where p is the pressure difference across the fabric, which is assumed to be constant.

Substituting from (23) in (24):

$$\frac{d}{dr} (r T_1 \sin \varphi) = pr$$

therefore
$$r T_1 \sin \varphi = \frac{pr^2}{2} + c \quad (25)$$

where c is a constant of integration. Substituting from equation (1) into equation (25)

$$T_1 = \frac{\lambda r}{\left(\lambda - 1 + \frac{r^2}{a^2}\right)} \left\{ \frac{p}{2} + \frac{c}{r^2} \right\} \quad (26)$$

and from (23)

$$T_2 = \frac{2\lambda r}{\left(\lambda - 1 + \frac{r^2}{a^2}\right)^2} \left\{ (\lambda - 1) \frac{p}{2} - \frac{c}{a^2} \right\}. \quad (27)$$

It is usual to determine the constant of integration c by considering the equilibrium of the axial forces acting on the system.

(i) For a parachute without vent or axial cord:

$$2\pi r T_1 \sin \varphi = p\pi r^2. \quad (28)$$

Evaluating this at $r = a$, $\varphi = \pi/2$ and equating the value for T_1 at $r = a$ with that given by (26):

$$\frac{pa}{2} = a \left\{ \frac{p}{2} + \frac{c}{a^2} \right\}$$

and hence

$$c = 0. \quad (29)$$

(ii) For a parachute with a vent of radius b but no axial cord:

$$2\pi r T_1 \sin \phi = p\pi(r^2 - b^2). \quad (30)$$

Hence

$$\frac{p(a^2 - b^2)}{2a} = a \left\{ \frac{p}{2} + \frac{c}{a^2} \right\}$$

and

$$c = -\frac{pb^2}{2}. \quad (31)$$

(iii) For the parachute with an axial cord:

$$2\pi r T_1 \sin \phi + T_c = p\pi r^2 \quad (32)$$

where T_c is the tension in the axial cord. When $\phi = 0$:

$$T_c = p\pi a^2(1 - \lambda); \quad (33)$$

and when $\phi = \frac{\pi}{2}$:

$$2\pi a T_1(r=a) + p\pi a^2(1 - \lambda) = p\pi a^2$$

therefore $T_1(r=a) = \frac{p\lambda a}{2} = a \left\{ \frac{p}{2} + \frac{c}{a^2} \right\}$ from (26).

Hence

$$c = \frac{pa^2}{2} (\lambda - 1). \quad (34)$$

It is important to note that, as a consequence of equation (34), the circumferential tension given by (27) is zero. The solid parachute with an axial cord is thus on the verge of crinkling and it is to be expected that it would be easily distorted by external aerodynamic forces resulting from, for example, gusts of wind.

It is also possible to obtain the value for c for the annular parachute with both central and outer peripheral cords; the value depends on the inner radius of the annulus and the angle the central cords make with the axis, together with the number of cords used.

Equations (26) and (27) reveal several interesting features. For the parachute without vent or axial cord

$$T_1 = \frac{\lambda pr}{2\left(\lambda - 1 + \frac{r^2}{a^2}\right)} \quad (35)$$

$$T_2 = \frac{\lambda(\lambda - 1)pr}{\left(\lambda - 1 + \frac{r^2}{a^2}\right)^2} \quad (36)$$

If the parachute is on the verge of crinkling and is as flat as possible the circumferential tension T_2 must be zero, this implies from (36) that $\lambda = 0$ or $\lambda = 1$, but $\lambda = 0$ is inadmissible (see para.2) and hence $\lambda = 1$ and the parachute takes up the Taylor shape. With $\lambda = 1$ it can be seen from equation (35) that the generator tension T_1 is always infinite when $r = 0$ i.e. at the canopy apex; in practice this is not possible but there is a high stress concentration at this point which is relieved to some extent by the elasticity of the fabric¹⁰. To avoid the stress concentration the parachute can be made slightly conical so that $\lambda > 1$; the stress at $r = 0$ is then theoretically zero and although the parachute is not on the verge of crinkling the circumferential tension, which must exist with $\lambda \neq 1$, is always positive and can be kept small by a suitable choice of λ . Similarly the inclusion of a vent helps to reduce the stress concentration near the apex of the canopy; in this case, for the circumferential stress to be zero, from equations (27) and (31):

$$T_2 = \frac{2\lambda r}{\left(\lambda - 1 + \frac{r^2}{a^2}\right)^2} \left\{ (\lambda - 1) \frac{p}{2} + \frac{pb^2}{2a^2} \right\} = 0$$

for $r \geq b$. This equation is satisfied if $\lambda = 0$, which is excluded, or

$$\lambda = 1 - \frac{b^2}{a^2}.$$

The generator tension T_1 , with this value for λ , is

$$T_1 = \frac{a^2 - b^2}{r} \frac{p}{2} \quad (37)$$

and remains finite when r tends to b which is the minimum possible value for r . The canopy equation is

$$\sin \phi = \frac{r^2 - b^2}{a^2 - b^2}$$

and this shows that the canopy is quite flat at $r = b$ ($\phi = 0$) where the vent commences. Whilst the stress given by (37) still increases near the vent this is not so serious as that in the Taylor shape.

It is desirable to have a slight positive circumferential tension in the fabric so that there is some resistance to distortion of the canopy shape by external forces; with zero or negative tension the canopy is prone to a form of instability in which the gores cling together and only partial inflation takes place. This should be overcome by making parachutes slightly conical.

3.2 The surface area of the fabric

In the solid fabric construction the canopy is assumed to form a surface of revolution and the surface area A is given by

$$A = 2\pi \int r ds = 2\pi \int \frac{r dr}{\cos \phi} .$$

Using equation (1)

$$\begin{aligned} A &= 2\pi a^2 \lambda \int \frac{\frac{r}{a} d\left(\frac{r}{a}\right)}{\sqrt{\left\{1 - \left(\frac{r}{a}\right)^2\right\} \left\{2\lambda - 1 + \frac{r^2}{a^2}\right\}}} \\ &= 2\pi a^2 \lambda \left[-\sin^{-1} \left\{ \frac{1 - \left(\frac{r}{a}\right)^2}{2\lambda} \right\}^{\frac{1}{2}} \right]_{r_0/a}^{r/a} \end{aligned} \quad (38)$$

where the integral is evaluated between appropriate limits.

As an example, the area of the Taylor shape ($\lambda = 1$) from the apex, $r = 0$, to the maximum diameter, $r = a$, is

$$A_{\lambda=1} = 2\pi a^2 \left\{ -\sin^{-1} 0 + \sin^{-1} \frac{1}{\sqrt{2}} \right\} = \frac{\pi a^2}{2} .$$

It is of interest to determine the particular design in which the surface area of fabric is a minimum. Consider only those canopies which meet the axis of symmetry, i.e. those for $\lambda > \frac{1}{2}$, and the surface area lying between $r = 0$ and $r = a$; it is assumed that below $r = a$ all canopies require approximately the same amount of fabric before the peripheral hem and this particular area is ignored.

Between $r = 0$ and $r = a$ the fabric surface area is

$$A = 2\pi a^2 \lambda \sin^{-1} \sqrt{\frac{1}{2\lambda}}.$$

For a critical value

$$\frac{dA}{d\lambda} = 2\pi a^2 \left\{ \sin^{-1} \sqrt{\frac{1}{2\lambda}} - \frac{1}{2\sqrt{2\lambda-1}} \right\} = 0.$$

The relevant root of $\frac{dA}{d\lambda} = 0$, which gives a minimum for A , is found graphically to occur when $\sqrt{\frac{1}{2\lambda}} \doteq 0.92$ or $\lambda \doteq 0.5907$. The canopy using the minimum fabric

area is thus one with an axial cord and its surface area between $r = 0$ and $r = a$ is $4.336a^2$. If this is compared with a Taylor shape parachute with the same inflated diameter i.e. drag area of πa^2 and fabric surface area of $\frac{\pi a^2}{2} = 4.935a^2$, the canopy with $\lambda = 0.5907$ represents a saving in fabric of about 13%; the total saving including the fabric between $r = a$ and the peripheral hem would be somewhat less than this and probably about 8-10%. If it is assumed that the drag coefficients of the Taylor shape and the canopy with an axial cord are the same under identical conditions, an increase in drag of about 13%, corresponding to a decrease of about 6% in the descent speed, might be expected from the canopy with $\lambda = 0.5907$ over the Taylor shape with the same fabric surface area. Some experimental evidence tending to support these conclusions appears in Ref.4; a direct comparison is not possible since the experiments were conducted by varying the length of the axial cord, and hence the parachute shape, on a parachute with cords over the canopy.

The Taylor shape was originally suggested¹ as that which would be of minimum bulk but from the present analysis it appears that the parachute with an axial cord and $\lambda = 0.5907$ is an improvement; however only conventional flat parachutes were considered in Ref.1. The process of minimising the bulk of a parachute could be carried further; one would expect an annular parachute, capped over the vent by a canopy with $\lambda = 0.5907$ and with an axial cord, to use a smaller fabric area for a given inflated diameter than the parachute with $\lambda = 0.5907$ on its own, and by adding further annular rings it may be possible to improve the ratio of fabric area to drag area even more. The improvements, if any, to be expected from modifications of this nature would probably be marginal; both the Taylor shape and the parachute with an axial cord are on the verge of crinkling (in the solid construction) and are liable to the instability mentioned in para.3.1; the presence of axial cords can also result in canopy malfunctions since they prevent total inversion in the case of a blown periphery. Research on parachutes with axial cords seems to have ceased at the end of World War II and very little data are available with regard to such factors as opening characteristics and stability and it is difficult to make comparisons; if there is a requirement for a particularly

low bulk parachute the more sophisticated experimental techniques now available should enable an assessment to be made. It may be added that the axial cord probably reduced the tendency for a parachute to breathe; breathing is known to produce a considerable variation in descent speed - in the case of the man carrying parachute this is of the order of ± 3 ft/sec with a mean descent speed of 16 ft/sec - and this is a contributory factor in landing injuries and damage.

3.3 The volume enclosed by the canopy

The volume enclosed by the canopy is given by

$$V = \int \pi r^2 dx = \int \pi r^2 \tan \phi dr .$$

Using equation (1)

$$V = \pi a^3 \int \frac{\left(\lambda - 1 + \frac{r^2}{a^2} \right) \frac{r^2}{a^2}}{\sqrt{\left\{ 1 - \left(\frac{r}{a} \right)^2 \right\} \left\{ 2\lambda - 1 + \frac{r^2}{a^2} \right\}}} d \left(\frac{r}{a} \right) . \quad (39)$$

Care is needed to ensure the regions of integration give the volume interior to the canopy and it is often necessary to separate the volume into a sum of integrals taken between several limits with the correct signs for each part of the total volume. The method of integration is briefly outlined in Appendix 1 and there are two separate cases: with $\lambda \geq \frac{1}{2}$,

$$V = -\pi a^3 \left[\left(\frac{1-\lambda}{3} \right) \sqrt{2\lambda} E \left(\cos^{-1} \frac{r}{a}, \frac{1}{\sqrt{2\lambda}} \right) + \left(\frac{2\lambda-1}{6} \right) \sqrt{2\lambda} F \left(\cos^{-1} \frac{r}{a}, \frac{1}{\sqrt{2\lambda}} \right) + \frac{1}{3} \frac{r}{a} \sqrt{\left\{ 1 - \left(\frac{r}{a} \right)^2 \right\} \left\{ 2\lambda - 1 + \left(\frac{r}{a} \right)^2 \right\}} \right]_{r_0/a}^{r/a} \quad (40)$$

taken between appropriate limits; and with $0 < \lambda \leq \frac{1}{2}$,

$$V = -\pi a^3 \left[\left(\frac{1-\lambda}{3} \right) E(\zeta, \sqrt{2\lambda}) - \left(\frac{1-2\lambda}{3} \right) F(\zeta, \sqrt{2\lambda}) + \frac{1}{3} \frac{r}{a} \sqrt{\left\{ 1 - \left(\frac{r}{a} \right)^2 \right\} \left\{ \left(\frac{r}{a} \right)^2 - (1-2\lambda) \right\}} \right]_{r_0/a}^{r/a} \quad (41)$$

between appropriate limits.

For the Taylor shape with $\lambda = 1$, the volume enclosed between the maximum diametral plane, $r = a$, and the apex is

$$\begin{aligned}
 V_{\lambda=1} &= -\pi a^3 \left\{ \frac{\sqrt{2}}{6} F\left(0, \frac{1}{\sqrt{2}}\right) - \frac{\sqrt{2}}{6} F\left(\frac{\pi}{2}, \frac{1}{\sqrt{2}}\right) \right\} \\
 &= \frac{\pi a^3 \sqrt{2}}{6} \times 1.8541 = 0.437 \pi a^3 .
 \end{aligned}$$

For the parachute with an axial cord and $\lambda = 0.5907$ the volume enclosed between $r = 0$ and $r = a$ is found to be $0.284 \pi a^3$; and for the conical parachute with a semi-vertical angle of 60° ($\lambda = 2$) the corresponding volume is $0.707 \pi a^3$. To these volumes must be added the volume contained in the skirt below $r = a$ which can be assumed constant for a given inflated diameter.

Whilst the volume of air contained in the canopy has no gravitational effect it does contribute to the inertia of the canopy which is of importance in considerations of stability: there are indications that stability is considerably improved as the canopy volume increases, against this must be balanced the facts that the large volume conical canopy requires more fabric and is slower in opening. It is desirable that experiments should be made to determine how canopy volume affects stability and opening; a deep conical canopy, with $\lambda = 2$ say, seems to offer several advantages in that the circumferential tension in the fabric is always positive, there is no stress concentration at the apex, the inertia of the canopy and contained air is high and should therefore produce less tendency for the parachute to breathe or oscillate laterally, and the opening shock should be low on account of the slow filling time for the canopy.

4. THE CORDS OVER CANOPY DESIGN

In this design, in the case of a parachute, the rigging lines are continued from the peripheral hem and run right over the apex of the canopy. The object is to relieve the stress in the fabric by having the cords taut in comparison with it and thus bearing much of the load; a stronger canopy than that given by the solid fabric construction is thus produced.

For the canopy to form a surface of revolution any cords passing over it must be slack in comparison with the fabric and can perform no useful function since they then might as well terminate at the peripheral hem. If the cords are made tighter than the fabric the canopy no longer forms a surface of revolution and the gore fabric bows out between adjacent cords. The tension in the fabric produces a force component to support the tension in the cords and it is possible to arrange this so that the circumferential tension in the fabric is approximately constant over the whole canopy. The basic assumption made in the design theory is that by gathering the gore fabric along the cords the stress in the generator direction can be made negligible so that only circumferential tension exists in the fabric, the cords bearing all the load in the generator direction. The problem essentially consists of finding the shape taken up by the cords and then determining the shape of the gore to be cut from a plane sheet of fabric which, when fitted, satisfies the assumptions of the theory. A method for determining the gore shape for the parachute has been given in Ref.2; this gore is generated by a circle of constant radius lying in the plane containing the normals to a pair of adjacent generator cords at corresponding points equidistant from the vertex and passing through these points, except for crinkles the gore surface is swept out by the circle as it passes down the cords from the vertex to the peripheral hem.

In Ref.2 which only concerns parachutes without vent or axial cord, it is shown that the cords over the canopy take up approximately the Taylor shape of equation (2); in an Appendix to Ref.5 a more accurate approach is made to determining the shape which takes into account the bowing out of the fabric between the cords, and shows that, depending on the number of cords, the shape they take up is slightly conical and is given by a member of the family of curves represented by equation (1). According to the type of parachute and the loading the shapes taken up by the cords can, in general, be represented by equation (1) with the appropriate values for λ . It is not intended to reproduce here the whole of the theory of the cords over canopy construction; for parachutes without vent or axial cord the reader is referred to Ref.2 and for parachutes with an axial cord to Ref.4. For a more general discussion covering a wide range of values of λ Ref.5 gives full details of the derivation of the cord and gore shapes. In this Note it is assumed that the cord shape is given by equation (1) and the equations for calculating particular gore shapes to satisfy the assumptions are only given.

It is shown in Ref.5, with a slight difference in notation, that if the radius of the gore generating circle is h , and the gore length measured along the mid-gore line is S , then the semi-gore width w is given by

$$w = h \sin^{-1} \left(\frac{r}{h} \sin \frac{\pi}{n} \right) \quad (42)$$

where n is the number of cords, and the length of the gore, for the case where $\lambda \geq \frac{1}{2}$, by

$$\frac{S-s}{a} = \frac{\sin^2 \frac{\pi}{n}}{\lambda} \int_0^{r/a} \frac{\left\{ 1 - \lambda + \frac{a}{h} \lambda \left(\frac{r}{a} \right) - \left(\frac{r}{a} \right)^2 \right\} \left(\frac{r}{a} \right)^2}{\sqrt{\left\{ 1 - \left(\frac{r}{a} \right)^2 \right\} \left\{ 2\lambda - 1 + \left(\frac{r}{a} \right)^2 \right\}}} d \left(\frac{r}{a} \right) \quad (43)$$

where s/a is given by equation (8). The method of evaluating the integral in (43) is given in Appendix 1 and the result is

$$\begin{aligned} \frac{S-s}{a} = \sin^2 \frac{\pi}{n} & \left[\left(\frac{1-\lambda}{3} \right) \sqrt{\frac{2}{\lambda}} E \left(\cos^{-1} \frac{r}{a}, \sqrt{\frac{1}{2\lambda}} \right) + \right. \\ & + \left(\frac{2\lambda-1}{6} \right) \sqrt{\frac{2}{\lambda}} F \left(\cos^{-1} \frac{r}{a}, \sqrt{\frac{1}{2\lambda}} \right) + \\ & + \left(\frac{1}{3\lambda} \frac{r}{a} - \frac{a}{2h} \right) \sqrt{\left\{ 1 - \left(\frac{r}{a} \right)^2 \right\} \left\{ 2\lambda - 1 + \left(\frac{r}{a} \right)^2 \right\}} - \\ & \left. - \frac{a}{h} (1-\lambda) \sin^{-1} \left\{ \frac{1 - \left(\frac{r}{a} \right)^2}{2\lambda} \right\}^{\frac{1}{2}} \right]_0^{r/a} \quad (44) \end{aligned}$$

Similarly, with $0 < \lambda \leq \frac{1}{2}$

$$\frac{S - s}{a} = \frac{\sin^2 \frac{\pi}{n}}{\lambda} \int_{r_1/a}^{r/a} \frac{\left\{ 1 - \lambda + \frac{a}{h} \lambda \left(\frac{r}{a} \right) - \left(\frac{r}{a} \right)^2 \right\} \left(\frac{r}{a} \right)^2}{\sqrt{\left\{ 1 - \left(\frac{r}{a} \right)^2 \right\} \left\{ \left(\frac{r}{a} \right)^2 - (1 - 2\lambda) \right\}}} d \left(\frac{r}{a} \right) \quad (45)$$

where s/a is given by equation (14).

On evaluating this integral the result obtained is

$$\begin{aligned} \frac{S - s}{a} = \sin^2 \frac{\pi}{n} & \left[\left(\frac{1 - \lambda}{3\lambda} \right) E(\zeta, \sqrt{2\lambda}) - \right. \\ & - \left(\frac{1 - 2\lambda}{3\lambda} \right) F(\zeta, \sqrt{2\lambda}) + \\ & + \left(\frac{1}{3\lambda} \frac{r}{a} - \frac{a}{2h} \right) \sqrt{\left\{ 1 - \left(\frac{r}{a} \right)^2 \right\} \left\{ \left(\frac{r}{a} \right)^2 - (1 - 2\lambda) \right\}} - \\ & \left. - \frac{a}{h} (1 - \lambda) \sin^{-1} \left\{ \frac{1 - \left(\frac{r}{a} \right)^2}{2\lambda} \right\}^{\frac{1}{2}} \right]_{r_1/a}^{r/a} . \quad (46) \end{aligned}$$

When the values of a/h and n have been chosen the gore shape may be worked out using equation (42) and either equation (44) or (46) depending on the value of λ .

Consideration of the equilibrium of the axial forces determines the tension in the cords and since it is assumed in the theory that the pressure difference across the fabric is constant and the tension in the fabric in the generator direction is zero the relation between hoop stress and pressure is approximately

$$\frac{T_2}{h} = p , \quad (47)$$

for the radius of curvature of the fabric in the circumferential direction is h if the elasticity of the fabric is neglected. The equation for the equilibrium of the axial forces also provides a relation between the pressure difference p , the loading and the geometric characteristics of the parachute which, in conjunction with equation (47), enables an estimate to be made of the tensile strength required in the fabric.

The value of a/h determines the fullness of the gores. If the number of cords for a parachute of maximum radius, a , is fixed, then the gore width must exceed the minimum required to cover the surface. For relatively small increases of width the rate of increase in the curvature is substantial but falls progressively. Since, for a given pressure difference, the tension T_2 and h are proportional, initial small increases in fullness of the gore enable the tensions, and consequently the fabric weight and thickness, to be reduced. The exact relation between the tension and fabric thickness cannot be formally represented for analytic use and the question of determining an optimum value for a/h has never been rigorously pursued. There is an element of diminishing returns as the value of a/h is increased and, in practice, values about two (2) have been chosen.

It should be emphasised that the approximate stress analyses given in this Note, for both types of construction, are only applicable to parachutes which are fully inflated and in steady descent; the assumption of constant pressure difference is then reasonable.

5 CONCLUSIONS

An analysis has been given of the shapes represented by the equation

$$\sin \phi = \frac{1}{\lambda} \left[\lambda - 1 + \frac{r^2}{a^2} \right]$$

with particular reference to those factors which may be useful in parachute design both in the solid fabric and cords over the canopy constructions. The equation is shown to give a range of shapes including those taken up by conical, flat and annular parachutes and those with axial cords.

There is apparently no simple physical meaning for the parameter λ ; in any parachute it is largely determined by extraneous features: a particular shape may be required; only certain materials may be available; the parachute may have to occupy a fixed spatial region so as not to interfere with the structure to which it is attached; it may have to occupy a certain bulk and so-on. No rule can be given enabling a designer to choose a particular λ , this can only be decided in the light of experimental evidence of the most suitable parachute to perform a particular task taking into account any extraneous features.

Approximate methods for calculating the fabric stresses in the solid construction show that it is desirable, in order to avoid serious stress concentrations and provide some resistance to deformation by external forces, to make parachutes slightly conical. Consideration of the fabric surface area required for the various canopy shapes in the solid construction shows that the minimum amount of fabric is used by a parachute with an axial cord and $\lambda = 0.5907$, this gives about 1% more drag than a Taylor shape of the same fabric surface area; some of the disadvantages of the parachute with an axial cord are remarked on. The volume enclosed in canopies of solid fabric construction is calculated and that of the conical parachute with $\lambda = 2.0$ shown to be considerably higher than that of a Taylor shape with the same inflated diameter; this has the advantage of increasing the inertia of the system and promoting stability but the disadvantage of requiring more fabric. It is concluded that experiments on the effects of canopy volume and shape on stability and opening are desirable and that the deep conical parachute merits particular investigation.

LIST OF SYMBOLS

A	fabric surface area in the solid construction
$E(\theta, k)$	the Legendre elliptic integral of the 2nd kind
$F(\theta, k)$	the Legendre elliptic integral of the 1st kind
S	arc length measured along the mid-gore line of the fabric in the cords over canopy design
T_1	generator tension
T_2	circumferential or hoop tension
T_c	axial cord tension
V	volume enclosed by the canopy in the solid construction
a	maximum radius of the canopy
b	radius of the canopy vent
c	a constant of integration
(In Appendix 1 a, b and c are not used in these contexts)	
h	radius of the gore generating circle
k	modulus of the elliptic integrals
k'	the complementary modulus defined by $k^2 + k'^2 = 1$
n	number of cords
p	constant pressure difference across the fabric
r	the radial coordinate
s	arc length
w	the semi-gore width
x	the axial coordinate
ζ	defined by equation (15)
θ	argument of the elliptic integrals
λ	a parameter
ξ	defined by equation (12)
ϕ	the angle made by the tangent to the curve with a plane normal to the axis of symmetry

LIST OF REFERENCES

<u>No.</u>	<u>Author</u>	<u>Title, etc.</u>
1	Jones, R. (Editor)	On the aerodynamic characteristics of parachutes. A.R.C. R&M 862. June, 1923.
2	Stevens, G.W.H. Johns, T.F.	The theory of parachutes with cords over the canopy. A.R.C. R&M 2320. July, 1942.
3	Richards, G.J.	The theory of a parachute with a central shroud line and zero circumferential tension. R.A.E. Report No. EXE 129. (Unpublished) July, 1942.
4	Johns, T.F.	Parachutes with an axial cord as well as cords over the canopy. A.R.C. R&M 2336. February, 1944.
5	Lester, W.G.S.	The statics of a symmetric inflatable lifting system. R.A.E. Tech. Note No. Mech. Eng. 356. July, 1962. A.R.C. 24,501. July, 1962.
6	Hancock, H.	Elliptic integrals. Dover Publications Inc. New York 1958. (Reprint of 1st Edition of 1917.)
7	Bowman, F.	Introduction to elliptic functions, with applications. Wiley. New York 1953.
8	Jahnke-Emde-Lösch	Tables of higher functions. McGraw Hill. New York 1960. 6th Edition.
9	Spenceley, G.W. & R.M.	Smithsonian elliptic functions tables. Smithsonian Inst. Washington. (Smithsonian Miscellaneous Collection, Vol.109.) 1947.
10	Duncan, W.J. Stevens, G.W.H. Richards, G.J.	Theory of the flat elastic parachute. A.R.C. R&M 2118. March, 1942.
11	Byrd, P.F. Friedman, M.D.	Handbook of elliptic integrals for engineers and physicists. Springer-Verlag, Berlin 1954.

APPENDIX 1

ELLIPTIC INTEGRALS

The Legendre elliptic integrals of the first and second kind respectively are defined by the relations

$$F(\theta, k) = \int_0^{\theta} \frac{d\psi}{\sqrt{1 - k^2 \sin^2 \psi}}$$

$$E(\theta, k) = \int_0^{\theta} \sqrt{1 - k^2 \sin^2 \psi} \, d\psi .$$

$E(\theta, k)$ and $F(\theta, k)$ are usually tabulated in terms of θ and α , where $k = \sin \alpha$, for the ranges $0 \leq \theta \leq \pi/2$, $0 \leq \alpha \leq \pi/2$. The range of the tables can be extended by using the following relations:-

$$E(-\theta, k) = -E(\theta, k)$$

$$F(-\theta, k) = -F(\theta, k)$$

$$E(m\pi \pm \theta, k) = 2m E\left(\frac{\pi}{2}, k\right) \pm E(\theta, k)$$

$$F(m\pi \pm \theta, k) = 2m F\left(\frac{\pi}{2}, k\right) \pm F(\theta, k) .$$

In this Note most of the integrals involved can be evaluated using one or more standard forms.

With

$$a^2 + b^2 = c^2, \quad k = \frac{a}{c}$$

and

$$\Delta(\theta, k) = \sqrt{1 - k^2 \sin^2 \theta} ,$$

the required forms are:-

$$\int_x^a \frac{dt}{\sqrt{(a^2 - t^2)(b^2 + t^2)}} = \frac{1}{c} F(\theta, k) \quad (i)$$

$$\text{where } \cos \theta = \frac{x}{a} ;$$

$$\int_x^a \sqrt{\left(\frac{b^2 + t^2}{a^2 - t^2}\right)} dt = c E(\theta, k) \quad (\text{ii})$$

$$\text{where } \cos \theta = \frac{x}{a};$$

$$\int_x^c \frac{dt}{\sqrt{(t^2 - b^2)(c^2 - t^2)}} = \frac{1}{c} F(\theta, k) \quad (\text{iii})$$

$$\text{where } \Delta(\theta, k) = \frac{x}{c};$$

$$\int_x^c \frac{t^2 dt}{\sqrt{(t^2 - b^2)(c^2 - t^2)}} = c E(\theta, k) \quad (\text{iv})$$

$$\text{where } \Delta(\theta, k) = \frac{x}{c}.$$

The integral in equation (43) can be written as a combination of integrals of the type

$$\begin{aligned} C_m &= - \int \frac{t^m dt}{\sqrt{(1 - t^2)(k'^2 + k^2 t^2)}} = \int \frac{\cos^m \theta d\theta}{\sqrt{1 - k^2 \sin^2 \theta}} \\ &= \int \text{cn}^m u du \end{aligned}$$

where $t = \cos \theta = \text{cn } u$

and $k^2 + k'^2 = 1.$

Recurrence relations for evaluating C_m are given in Ref.11; the method of deriving these relations is given in Ref.6 but it should be noted that the relations quoted there are incorrect due to misprinting.

The integral in equation (45) can similarly be written in terms of integrals of the type

$$D_m = - \int \frac{t^m dt}{\sqrt{(1 - t^2)(t^2 - k'^2)}} = \int \text{dn}^m u du$$

where $t = \text{dn } u.$

Recurrence relations for evaluating D_m are again to be found in Ref.11. The integral in equation (39) for the cases $\lambda \geq \frac{1}{2}$ and $0 < \lambda \leq \frac{1}{2}$ is evaluated using these same recurrence relations.

APPENDIX 2

CANOPY, CORD AND GORE COORDINATES

The coordinates r/a and x/a for the canopy or cord shape are given in Tables 1 and 2. In order to determine the gore shape in the solid fabric construction values of s/a for the gore length are given and the gore width can be calculated from

$$\frac{2w}{a} = \frac{2\pi}{n} \left(\frac{r}{a} \right)$$

where n is the number of gores.

Table 1 is calculated for several cases where $\lambda > \frac{1}{2}$; the corresponding values for λ and $\sin^{-1} k = \sin^{-1} \sqrt{\frac{1}{2\lambda}}$ respectively are as follows:-

0.5156, 80°; 0.5664, 70°; 0.6667, 60°; 0.7500, 55°; 0.8522, 50°; 0.9055, 48°; 0.9347, 47°; 0.9664, 46°; 1.000, 45°; 1.210, 40°; 1.520, 35°; 2.000, 30°; and 2.799, 25°. The intervals for r/a are those corresponding to values of $\xi (= \cos^{-1} r/a)$ from $\xi = 90^\circ$, $r/a = 0$ to $\xi = 0$, $r/a = 1.0$ at intervals of 5° , these give the part of the curve lying between the point where it meets the axis and the points $r = a$, $\phi = \pi/2$; the continuation of the curve from $\phi = \pi/2$ onwards until the axis of symmetry is met again is a mirror image in the plane containing $r = a$ as is shown dotted in for the curve $\lambda = 0.5156$ in Fig.2. The curves shown plotted in Fig.2 are at intervals for $\sin^{-1} k$ of 5° from 25° to 60° and then at intervals from 60° to 80° of 10° .

Table 2 is calculated for three cases where $0 < \lambda < \frac{1}{2}$ and the curve does not meet the axis of symmetry. The corresponding values for λ and $\sin^{-1} k = \sin^{-1} \sqrt{2\lambda}$ are as follows:- 0.4849, 80°; 0.4415, 70°; and 0.3750, 60°. The intervals for r/a in each case are those corresponding to intervals of 10° from $\phi = -90^\circ$ to $\phi = +90^\circ$ and the continuation of the curve is a mirror image in the plane containing $r = a$ as shown dotted in for the case $\lambda = 0.3750$ in Fig.3; this figure shows the curves for the three values of λ .

Some examples of the gore shape for the solid fabric construction are shown in Fig.4. The gore shapes for $\lambda = 0.5156$, 1.00 and 2.00 are to fit canopies extending from a vertex $r = 0$ to the maximum radius $r = a$. The gore for $\lambda = 0.3750$ is that for $r/a = 0.5$ to $r/a = 1.0$ since the curve does not exist if $r/a < 0.5$.

TABLE 1

Coordinates for canopies with $\lambda > 4$

ξ	$\lambda = 0.5156$		$\lambda = 0.5664$		$\lambda = 0.6667$		$\lambda = 0.7500$		$\lambda = 0.8522$		$\lambda = 0.9055$		$\lambda = 0.9347$		$\lambda = 0.9664$		$\lambda = 1.0000$		$\lambda = 1.210$		$\lambda = 1.520$		$\lambda = 2.000$		$\lambda = 2.799$			
	r/a	s/a	x/a	s/a	x/a	s/a	x/c	s/a	x/c	s/a	x/c	s/c	x/a	s/a	x/a	s/c	x/a	s/a	x/a	s/a	x/a	s/a	x/a	s/a	x/a	s/a	x/a	
90	0.000	0.000	0.000	0.000	0.000	0.000	0.000	0.000	0.000	0.000	0.000	0.000	0.000	0.000	0.000	0.000	0.000	0.000	0.000	0.000	0.000	0.000	0.000	0.000	0.000	0.000	0.000	
85	0.087	0.246	-0.250	-0.102	-0.050	-0.031	0.089	-0.015	0.089	-0.015	0.088	-0.009	-0.006	0.087	-0.003	0.087	-0.003	0.087	-0.003	0.087	-0.003	0.087	-0.003	0.087	-0.003	0.087	-0.003	0.087
80	0.174	0.451	-0.416	-0.196	-0.096	-0.060	0.176	-0.028	0.176	-0.028	0.175	-0.015	-0.010	0.174	-0.004	0.174	-0.004	0.174	-0.004	0.174	-0.004	0.174	-0.004	0.174	-0.004	0.174	-0.004	0.174
75	0.259	0.613	-0.553	-0.276	-0.157	-0.085	0.262	-0.039	0.262	-0.039	0.260	-0.021	-0.012	0.259	-0.003	0.259	-0.003	0.259	-0.003	0.259	-0.003	0.259	-0.003	0.259	-0.003	0.259	-0.003	0.259
70	0.342	0.742	-0.652	-0.484	-0.339	-0.104	0.345	-0.044	0.345	-0.044	0.343	-0.021	-0.010	0.342	0.002	0.342	0.002	0.342	0.002	0.342	0.002	0.342	0.002	0.342	0.002	0.342	0.002	0.342
65	0.423	0.849	-0.722	-0.577	-0.387	-0.116	0.426	-0.044	0.426	-0.044	0.424	-0.017	-0.003	0.423	0.012	0.423	0.012	0.424	0.012	0.424	0.012	0.424	0.012	0.424	0.012	0.424	0.012	0.424
60	0.500	0.940	-0.770	-0.661	-0.420	-0.120	0.503	-0.038	0.503	-0.038	0.502	-0.006	0.010	0.502	0.025	0.502	0.025	0.503	0.025	0.503	0.025	0.503	0.025	0.503	0.025	0.503	0.025	0.503
55	0.574	1.020	-0.801	-0.738	-0.439	-0.117	0.578	-0.026	0.578	-0.026	0.577	0.010	0.028	0.578	0.045	0.579	0.045	0.580	0.045	0.580	0.045	0.580	0.045	0.580	0.045	0.580	0.045	0.580
50	0.643	1.091	-0.817	-0.807	-0.447	-0.106	0.650	-0.007	0.650	-0.007	0.650	0.032	0.032	0.651	0.072	0.652	0.072	0.655	0.072	0.655	0.072	0.655	0.072	0.655	0.072	0.655	0.072	0.655
45	0.707	1.156	-0.820	-0.872	-0.445	-0.088	0.719	0.018	0.719	0.018	0.720	0.060	0.060	0.722	0.103	0.724	0.103	0.727	0.103	0.727	0.103	0.727	0.103	0.727	0.103	0.727	0.103	0.727
40	0.766	1.215	-0.813	-0.932	-0.433	-0.063	0.785	0.049	0.785	0.049	0.783	0.094	0.094	0.790	0.140	0.793	0.140	0.797	0.140	0.797	0.140	0.797	0.140	0.797	0.140	0.797	0.140	0.797
35	0.819	1.271	-0.798	-0.989	-0.414	-0.032	0.850	0.085	0.850	0.085	0.854	0.133	0.133	0.857	0.182	0.861	0.182	0.866	0.182	0.866	0.182	0.866	0.182	0.866	0.182	0.866	0.182	0.866
30	0.866	1.323	-0.775	-1.042	-0.387	0.004	0.912	0.126	0.912	0.126	0.918	0.176	0.176	0.922	0.228	0.927	0.228	0.932	0.228	0.932	0.228	0.932	0.228	0.932	0.228	0.932	0.228	0.932
25	0.906	1.373	-0.746	-1.094	-0.355	0.045	0.973	0.172	0.973	0.172	0.980	0.224	0.224	0.985	0.251	0.991	0.251	0.998	0.251	0.998	0.251	0.998	0.251	0.998	0.251	0.998	0.251	0.998
20	0.940	1.421	-0.712	-1.144	-0.318	0.090	1.033	0.221	1.033	0.221	1.042	0.275	0.275	1.047	0.303	1.054	0.303	1.062	0.303	1.062	0.303	1.062	0.303	1.062	0.303	1.062	0.303	1.062
15	0.966	1.467	-0.673	-1.192	-0.278	0.139	1.091	0.273	1.091	0.273	1.102	0.329	0.329	1.109	0.358	1.116	0.358	1.125	0.358	1.125	0.358	1.125	0.358	1.125	0.358	1.125	0.358	1.125
10	0.985	1.512	-0.632	-1.240	-0.234	0.189	1.149	0.328	1.149	0.328	1.161	0.386	0.386	1.169	0.415	1.178	0.415	1.187	0.415	1.187	0.415	1.187	0.415	1.187	0.415	1.187	0.415	1.187
5	0.996	1.557	-0.589	-1.286	-0.189	0.193	1.206	0.384	1.206	0.384	1.220	0.444	0.444	1.229	0.474	1.239	0.474	1.249	0.474	1.249	0.474	1.249	0.474	1.249	0.474	1.249	0.474	1.249
0	1.000	1.601	-0.545	-1.333	-0.143	0.246	1.263	0.441	1.263	0.441	1.279	0.502	0.502	1.289	0.534	1.299	0.534	1.311	0.534	1.311	0.534	1.311	0.534	1.311	0.534	1.311	0.534	1.311

TABLE 2

Coordinates for canopies with $0 < \lambda < \frac{1}{2}$

φ	ζ	$\lambda = 0.4849$			$\lambda = 0.4415$			$\lambda = 0.3750$		
		r/a	s/a	x/a	r/a	s/a	x/a	r/a	s/a	x/a
-90	90	0.174	0.000	0.000	0.342	0.000	0.000	0.500	0.000	0.000
-80	85	0.194	0.235	-0.234	0.352	0.112	-0.111	0.506	0.065	-0.065
-70	80	0.244	0.431	-0.423	0.379	0.218	-0.213	0.522	0.129	-0.126
-60	75	0.309	0.585	-0.563	0.420	0.314	-0.301	0.548	0.190	-0.182
-50	70	0.379	0.709	-0.664	0.469	0.401	-0.372	0.581	0.248	-0.229
-40	65	0.451	0.811	-0.737	0.524	0.479	-0.427	0.620	0.303	-0.268
-30	60	0.522	0.898	-0.787	0.581	0.549	-0.467	0.662	0.354	-0.297
-20	55	0.591	0.974	-0.819	0.638	0.612	-0.494	0.705	0.402	-0.318
-10	50	0.656	1.042	-0.837	0.694	0.670	-0.509	0.748	0.447	-0.329
0	45	0.718	1.104	-0.842	0.747	0.723	-0.514	0.791	0.489	-0.333
10	40	0.774	1.160	-0.837	0.797	0.773	-0.509	0.831	0.530	-0.330
20	35	0.825	1.213	-0.824	0.842	0.820	-0.497	0.868	0.568	-0.319
30	30	0.870	1.263	-0.802	0.883	0.865	-0.478	0.901	0.605	-0.304
40	25	0.909	1.311	-0.775	0.918	0.908	-0.454	0.931	0.641	-0.283
50	20	0.942	1.356	-0.743	0.947	0.949	-0.425	0.955	0.676	-0.259
60	15	0.967	1.401	-0.707	0.970	0.989	-0.392	0.975	0.710	-0.231
70	10	0.985	1.444	-0.668	0.987	1.028	-0.356	0.989	0.743	-0.201
80	5	0.996	1.487	-0.626	0.997	1.067	-0.319	0.997	0.776	-0.169
90	0	1.000	1.529	-0.584	1.000	1.106	-0.280	1.000	0.809	-0.137

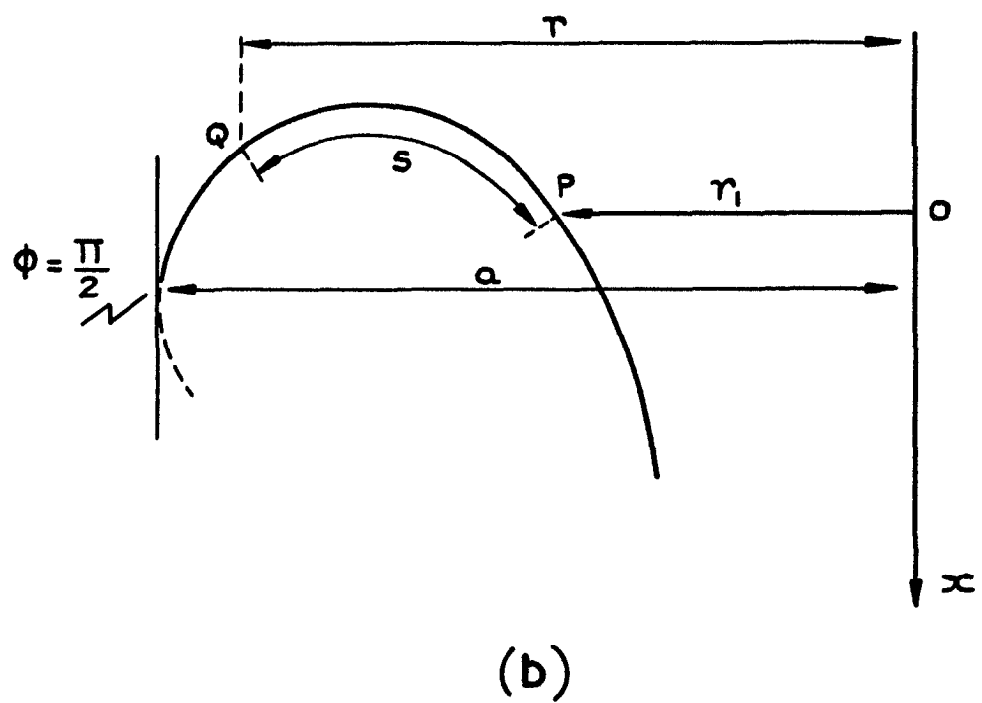
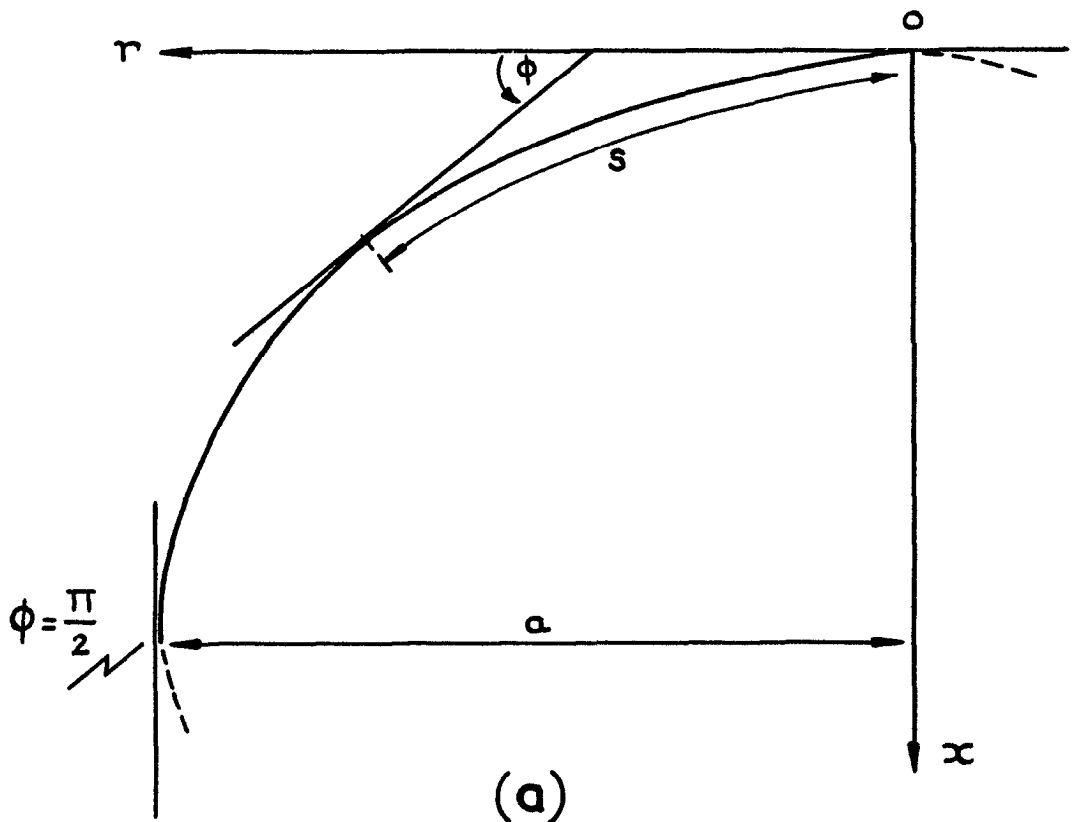


FIG. 1. (a - b) DIAGRAMS SHOWING THE NOTATION USED WHEN (a) $\lambda > \frac{1}{2}$ AND (b) $0 < \lambda < \frac{1}{2}$

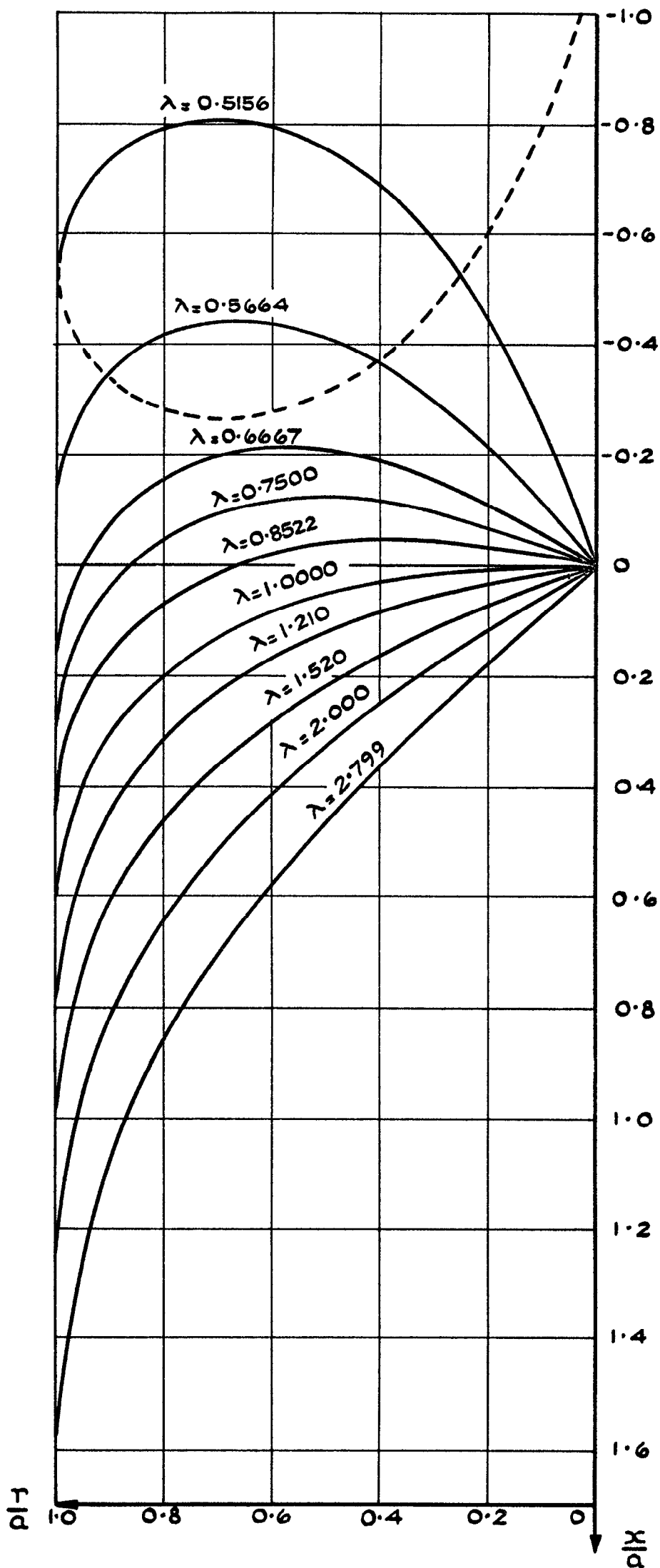


FIG. 2. CANOPY SHAPES FOR $\lambda > \frac{1}{2}$.

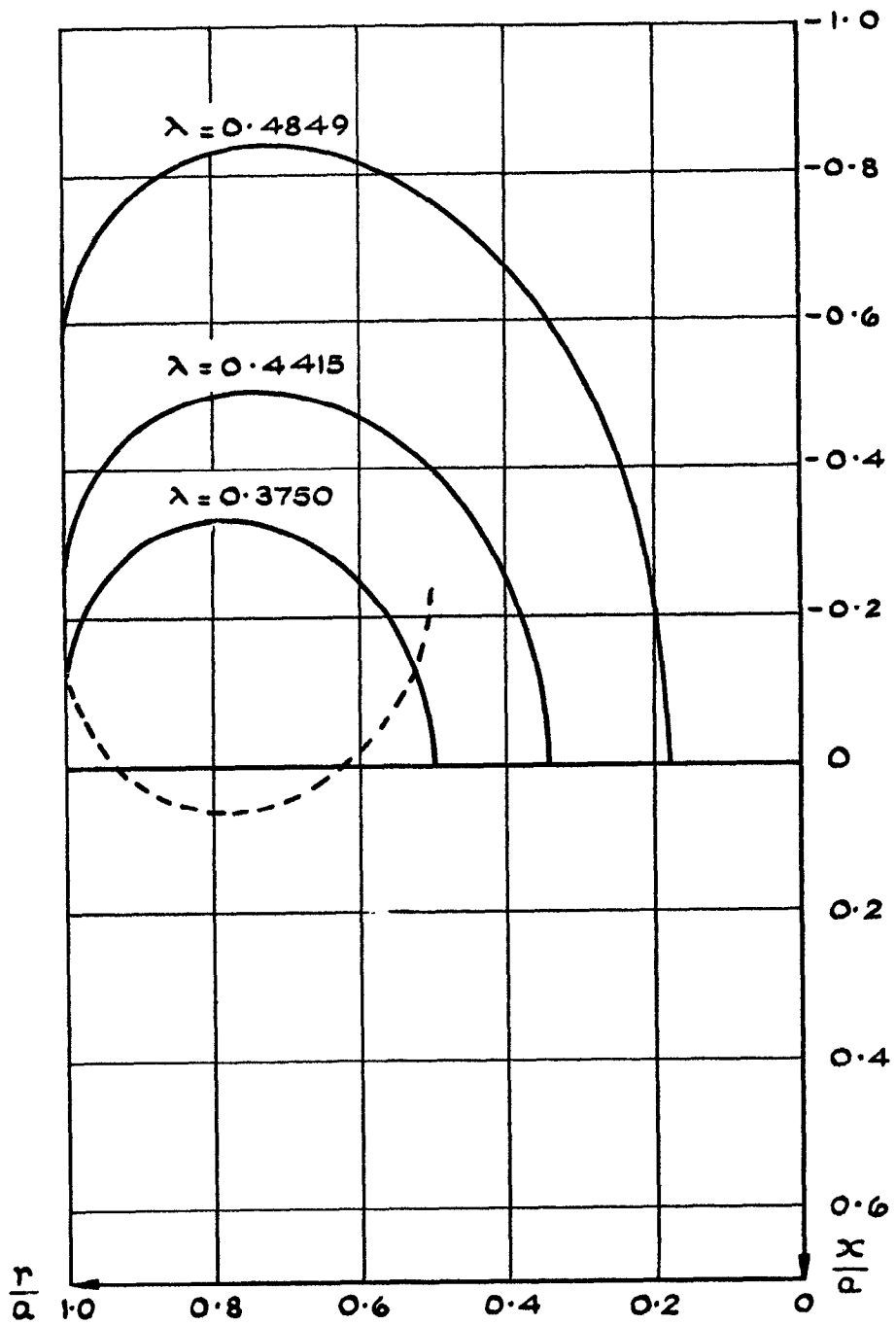


FIG.3. CANOPY SHAPES FOR $0 < \lambda < \frac{1}{2}$.

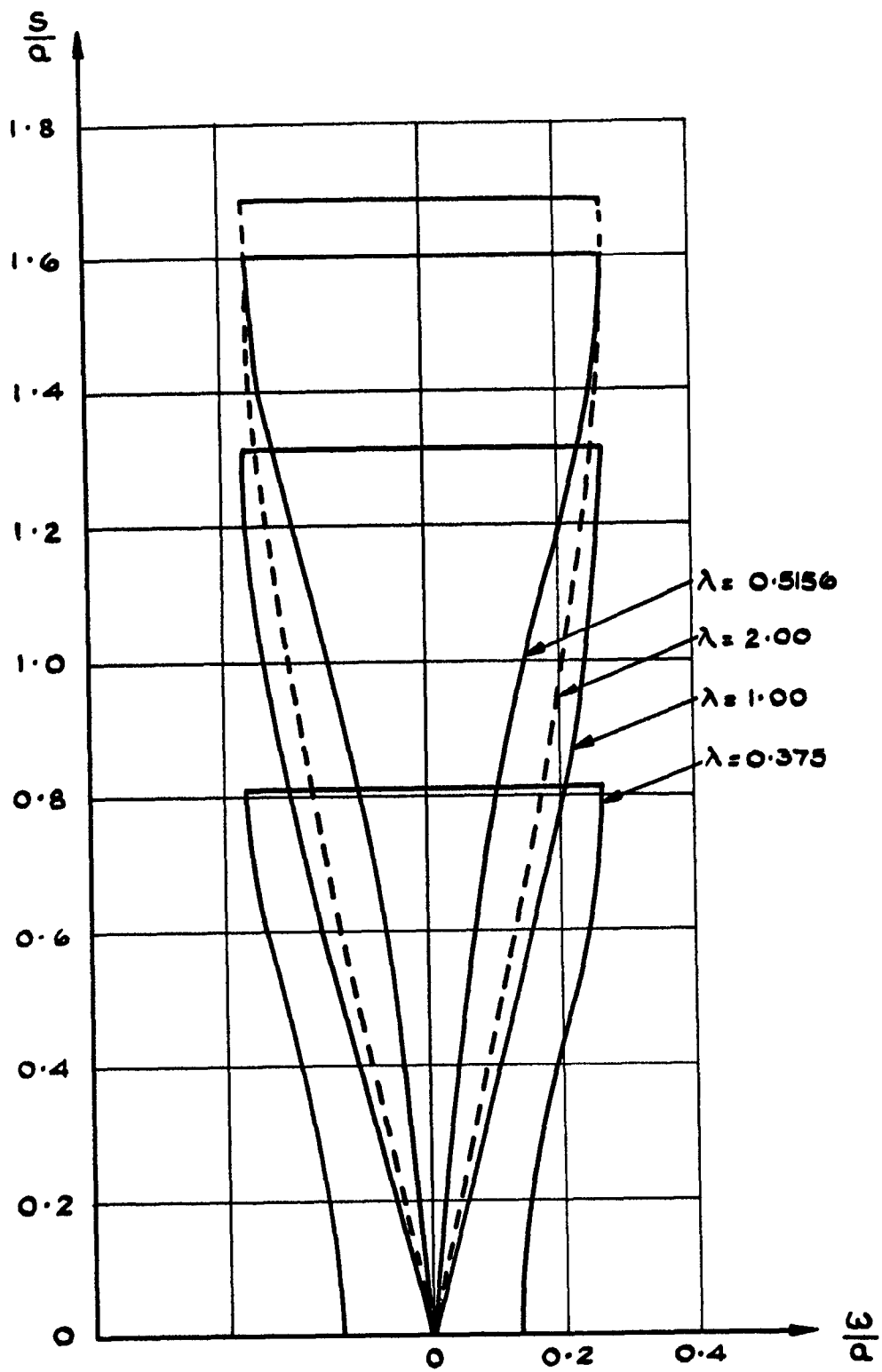


FIG. 4. GORE SHAPES FOR THE SOLID FABRIC CONSTRUCTION.

A.R.C. C.P. No.665

533,666,2:
516.4

A NOTE ON THE GENERALISATION OF ELASTIC CURVES REPRESENTING PARACHUTE SHAPES. Lester, W.G.S. July, 1962.

The Note gives a concise treatment of the theory of parachute canopy shapes and stresses. An analysis is made of the equation

$$\sin \phi = \frac{1}{\lambda} \left[\lambda - 1 + \frac{r^2}{a^2} \right]$$

where r is the radial distance measured from the axis of symmetry and a its maximum value; ϕ is the angle the tangent to the curve makes with a plane normal to the axis of symmetry and λ is a parameter. By varying

(Over)

A.R.C. C.P. No.665

533,666,2:
516.4

A NOTE ON THE GENERALISATION OF ELASTIC CURVES REPRESENTING PARACHUTE SHAPES. Lester, W.G.S. July, 1962.

The Note gives a concise treatment of the theory of parachute canopy shapes and stresses. An analysis is made of the equation

$$\sin \phi = \frac{1}{\lambda} \left[\lambda - 1 + \frac{r^2}{a^2} \right]$$

where r is the radial distance measured from the axis of symmetry and a its maximum value; ϕ is the angle the tangent to the curve makes with a plane normal to the axis of symmetry and λ is a parameter. By varying

(Over)

A.P.C. C.P. No.665

533,666,2:
516.4

A NOTE ON THE GENERALISATION OF ELASTIC CURVES REPRESENTING PARACHUTE SHAPES. Lester, W.G.S. July, 1962.

The Note gives a concise treatment of the theory of parachute canopy shapes and stresses. An analysis is made of the equation

$$\sin \phi = \frac{1}{\lambda} \left[\lambda - 1 + \frac{r^2}{a^2} \right]$$

where r is the radial distance measured from the axis of symmetry and a its maximum value; ϕ is the angle the tangent to the curve makes with a plane normal to the axis of symmetry and λ is a parameter. By varying

(Over)

λ a family of elastic curves is generated representing the shapes of flat, conical and annular parachutes and also those with an axial cord. General equations for calculating the fabric surface area and canopy volume in the solid fabric construction are included, together with equations for determining the gore shapes for both the cords over canopy and solid fabric constructions. An approximate analysis is given of the stress distribution in the two constructions. A parachute with an axial cord is shown to have the minimum bulk for a given inflated diameter but its merit on other parachute requirements is doubtful. Experiments are suggested to relate canopy shape and volume with stability and a deep conical parachute is thought to have several desirable stability characteristics.

λ a family of elastic curves is generated representing the shapes of flat, conical and annular parachutes and also those with an axial cord. General equations for calculating the fabric surface area and canopy volume in the solid fabric construction are included, together with equations for determining the gore shapes for both the cords over canopy and solid fabric constructions. An approximate analysis is given of the stress distribution in the two constructions. A parachute with an axial cord is shown to have the minimum bulk for a given inflated diameter but its merit on other parachute requirements is doubtful. Experiments are suggested to relate canopy shape and volume with stability and a deep conical parachute is thought to have several desirable stability characteristics.

λ a family of elastic curves is generated representing the shapes of flat, conical and annular parachutes and also those with an axial cord. General equations for calculating the fabric surface area and canopy volume in the solid fabric construction are included, together with equations for determining the gore shapes for both the cords over canopy and solid fabric constructions. An approximate analysis is given of the stress distribution in the two constructions. A parachute with an axial cord is shown to have the minimum bulk for a given inflated diameter but its merit on other parachute requirements is doubtful. Experiments are suggested to relate canopy shape and volume with stability and a deep conical parachute is thought to have several desirable stability characteristics.

C.P. No. 665

© *Crown Copyright 1963*

Published by
HER MAJESTY'S STATIONERY OFFICE

To be purchased from
York House, Kingsway, London w.c.2
423 Oxford Street, London w.1
13A Castle Street, Edinburgh 2
109 St. Mary Street, Cardiff
39 King Street, Manchester 2 -
50 Fairfax Street, Bristol 1
35 Smallbrook, Ringway, Birmingham 5
80 Chichester Street, Belfast 1
or through any bookseller

S.O. CODE No. 23-9013-65

C.P. No. 665